Figure Captions

Chapter 2

Fig. 2-1 OTFT device configurations. (a) Schematic cross section view of top contact device. (b) Schematic cross section view of bottom contact device.

Fig. 2-2 Schematic of operation of OTFT, showing a p-type semiconductor: + indicates a positive charge in semiconductor; - indicate a negatively charge. (a) no-bias (b) accumulation mode (c) depletion mode.

Fig. 2-3 Energy band diagrams (a) for a p-channel (pentacene) and (b) for a n-channel (NTCDA) OTFTs. The left side shows the devices at zero gate bias, while in the centre and in the right part the accumulation and depletion mode operation regimes are presented.

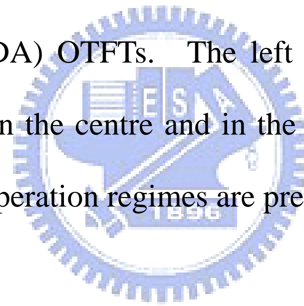

Chapter 3

Fig. 3-1 Schematic cross section view of MIS-Au/AlN/Si capacitors structure.

Chapter 4

Fig. 4-1 The AFM images of AlN films deposited at 250°C, 200°C, and 150°C are shown in Fig. (a), Fig. (b), and Fig. (c), respectively. The scanning size is fixed to be 5×5 μm^2. The rms roughness values are 0.43, 0.31, 0.17 nm, respectively.

Fig. 4-2 The leakage current of the Au/AlN/Si MIS structure as a function of the electric field and gate voltage. The inset is the capacitance measured from the same structure under various frequencies.

Fig. 4-3 The AFM images of AlN films deposited at Ar/N_2 ratio: 2/5, 2/7, 2/9 are shown in Fig. (a), Fig. (b), and Fig. (c), respectively. The scanning size is fixed to be 5×5 μm^2. The rms roughness values are 0.20, 0.21, 0.18 nm, respectively.

Fig. 4-4 The x-ray photoemission spectrum (XPS) signal form the AlN sample (different sputtering condition).

Fig. 4-5 The J-E plots of the Au/AlN/Si MIS structure from different Ar/N_2 flow rate in AlN sputtering process.

Fig. 4-6 (a) The leakage current from three MIS structures are plotted as a function of electric field in log(J) vs. log(E) plots and (b) in ln(J/E) vs. $(E)^{1/2}$ plot.

Fig. 4-7 The AFM images of AlN films deposited at 250°C, 200°C, and 150°C are shown in Fig. (a), Fig. (b), and Fig. (c), respectively. The corresponding AFM images of pentacene films grown on the 250°C, 200°C, and 150°C AlN dielectrics are shown in Fig. (d), Fig. (e), and Fig. (f). The scanning size is fixed to be 5×5 μm^2.

Fig. 4-8 The transfer characteristic of the OTFTs with 150°C, 200°C, and 250°C AlN gate dielectric. The drain bias is -3 V.

Fig. 4-9 The plot of square root of drain current versus the gate voltage when the drain bias is -7 V.

Fig. 4-10 The output characteristic of the OTFTs with 150°C AlN gate dielectric.

Fig. 4-11 The output characteristic of the OTFTs with 200°C AlN gate dielectric.

Fig. 4-12 The output characteristic of the OTFTs with 250°C AlN gate dielectric.

1896

Fig. 4-13 The field effect mobility of OTFTs with 150°C, 200°C, and 250°C AlN gate dielectric. The drain bias is -3 V. The field effect mobility is extracted from the linear region transconductance.

Fig. 4-14 The cross-sectional SEM image of AlN dielectric.

Fig. 4-15 The leakage current of MIS structure as a function of electric field and gate voltage. The inset is the capacitance measured from the same structure under various frequencies.

Fig. 4-16 (a) The transfer characteristics of AlN-OTFTs. The gate voltage was scanned from +1 V to -5 V. (b) The square root of drain current vs. the gate voltage.

Fig. 4-17 The output characteristics of AlN-OTFTs.

Fig. 4-18 The AFM image of higher Ar/N_2 ratio sputtered AlN film. The scanning sized is $5\times5\ \mu m^2$.

Fig. 4-19 The AFM images of pentacene films grown at higher Ar/N_2 ratio AlN dielectrics. The scanning sized is $5\times5\ \mu m^2$.

Fig. 4-20 The leakage current of MIS structure as a function of electric field and gate voltage. The inset is the capacitance measured from the same structure under various frequencies.

Fig. 4-21 The cross-sectional SEM image of AlN dielectric with higher Ar/N_2 ratio.

Fig. 4-22 The transfer characteristics of AlN-OTFTs. The gate voltage was scanned from +1 V to -5 V.

Fig. 4-23 The square root of drain current vs. the gate voltage. The gate voltage was scanned from +1 V to -5 V.

Fig. 4-24 The output characteristics of OTFTs with higher Ar/N_2 ratio AlN films.

Fig. 4-25 The AFM image of room temperature sputtered AlN film. The

scanning sized is 5×5 μm^2.

Fig. 4-26 The AFM images of pentacene films grown on the room temperature AlN dielectrics. The scanning sized is 5×5 μm^2.

Fig. 4-27 The leakage current of MIS structure as a function of electric field and gate voltage. The inset is the capacitance measured from the same structure under various frequencies.

Fig. 4-28 The cross-sectional SEM image of room temperature AlN dielectric.

Fig. 4-29 The transfer characteristics of AlN-OTFTs. The gate voltage was scanned from +1 V to -5 V.

Fig. 4-30 The square root of drain current vs. the gate voltage. The gate voltage was scanned from +1 V to -5 V.

Fig. 4-31 The output characteristics of OTFTs with room temperature AlN films.